Angewandte Chemie International Edition

DOI: 10.1002/anie.201004929

Graphene

Layer-by-Layer Films of Graphene and Ionic Liquids for Highly Selective Gas Sensing[**]

Qingmin Ji,[*] Itaru Honma,[*] Seung-Min Paek, Misaho Akada, Jonathan P. Hill, Ajayan Vinu, and Katsuhiko Ariga[*]

Molecular sensing of useful or toxic substances has been extensively investigated and has revealed that well-designed host structures are essential for high sensitivities and selectivities. In addition to organic supramolecular hosts,[1] structure-controlled inorganic nanomaterials have become increasingly important in this area.[2] In particular, graphene has emerged as an important compound because of its homogeneous thickness and extended conjugated π-electronic structure.[3] Control of the spacing between graphene layers upon their reassembly should result in 2D cavities that are ideal for molecular discrimination, although this approach remains challenging. Fortunately, the high affinity between nanocarbons and certain kinds of ionic liquids has been previously reported[4] and guided us in our formulation of a solution to this problem. Consequently, we now introduce a method for the formation of graphene layers that are intercalated by ionic liquids. The layered structures are formed by in situ reduction of graphene oxide layers in the presence of nonvolatile ionic liquids, and subsequent electrostatic layer-by-layer (LbL) assembly[5] (Figure 1). We further demonstrate the use of layered graphene/ionic liquid (G–IL) composites on quartz crystal microbalances (QCM) for selective gas sensing. The nanospace formed between sp^2-hybridized carbon nanosheets has a higher affinity for toxic aromatic hydrocarbons than for their aliphatic analogues.

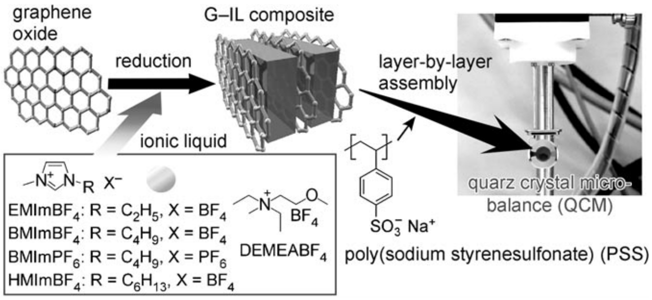

Figure 1. Schematic illustration of the preparation of graphene/ionic liquid (G–IL) composites and their LbL assembly on a quartz crystal microbalance (QCM).

Graphene oxide (GO) was prepared by oxidation of graphite under acidic conditions,[6] and subsequent reduction to form graphene (G) in the presence of ionic liquids in water.[7] The Raman spectra of both G prepared with 1-ethyl-3-methylimidazolium tetrafluoroborate ($EMImBF_4$, G–$EMImBF_4$, see Figure 1) and GO exhibit G-mode and D-mode peaks,[7] which arise from the vibration of sp^2-hybridized carbon atoms in a 2D hexagonal lattice with dangling bonds in disordered plane terminations, respectively.[8] The high energy G-mode peak of G–$EMImBF_4$ (1561 cm^{-1}) is more intense and blue-shifted relative to that of GO (1602 cm^{-1}), thus implying that the disorder of the graphene rings is suppressed during reduction. The XRD pattern of GO contains an intense 001 peak that corresponds to a *d* spacing of approximately 0.8 nm,[7] which is in accordance with the layer-to-layer distance estimated from AFM observations.[7] In contrast, the XRD pattern of G–$EMImBF_4$ contains a broad 002 graphitic diffraction peak, as well as many additional weak diffraction peaks, hence suggesting the intercalation of $EMImBF_4$ molecules into the G.[9] FT-IR measurements on G–$EMImBF_4$ also indicate the lack of a carbonyl stretching band (1750 cm^{-1}), whereas C−H stretching (2940 cm^{-1}) and deformation (1410 cm^{-1}) bands in addition to a new band at 1670 cm^{-1} appear. The latter band arises from the vibration of the intercalated imidazolium framework.[7] Thermogravimetric analysis (TGA) indicates that G–$EMImBF_4$ contains approximately 22 wt % organic compounds, according to the weight loss in the temperature range 200–500 °C.[7]

TEM images of G–$EMImBF_4$ (Figure 2 d, e) reveal thin-film structures composed of 2–4 graphene layers. The structures have an enlarged layer spacing compared with G prepared in the absence of ionic liquid (G–water, Figure 2 a and b) because of the intercalation of $EMImBF_4$. The mean layer spacing of G–$EMImBF_4$ was estimated to be approx-

---

[*] Dr. Q. Ji, M. Akada, Dr. J. P. Hill, Dr. A. Vinu, Prof. Dr. K. Ariga
World Premier International (WPI) Research Center for Materials Nanoarchitectonics (MANA)
National Institute for Materials Science (NIMS)
1-1 Namiki, Tsukuba 305-0044 (Japan)
Fax: (+81) 29-860-4832
E-mail: ARIGA.Katsuhiko@nims.go.jp
JI.Qingmin@nims.go.jp
Homepage: http://www.nims.go.jp/super/HP/home.htm
Dr. J. P. Hill, Prof. Dr. K. Ariga
JST, CREST
1-1 Namiki, Tsukuba 305-0044 (Japan)
Prof. Dr. I. Honma
Institute of Multidisciplinary Research for Advanced Materials
Tohoku University, Sendai 980-8577 (Japan)
E-mail: i.honma@tagen.tohoku.ac.jp
Dr. S.-M. Paek
Department of Chemistry, Kyungpook National University
Daegu, 702-701 (Korea)

[**] This work was supported in part by WPI Initiative, MEXT, JST, CREST, and JSPS. The authors thank Dr. Y. Nemoto for high-resolution TEM measurements.

Supporting information for this article is available on the WWW under http://dx.doi.org/10.1002/anie.201004929.

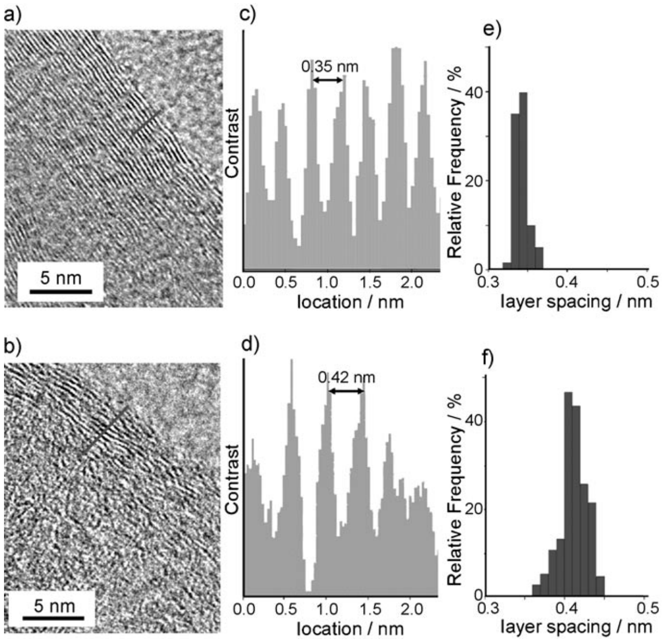

Figure 2. High-resolution TEM images of a) G reduced in water (G–water) and b) G reduced in the presence of $EMImBF_4$ (G–$EMImBF_4$). c, d) Cross-sections taken along the lines in (a) and (b), respectively. e, f) Statistical treatment of layer spacing distributions revealed average layer spacing for G–water (0.35 nm) and G–$EMImBF_4$ (0.42 nm).

imately 0.41 nm (Figure 2 f), while G–water was composed of more than 10 layers with a mean layer spacing of approximately 0.35 nm (Figure 2 c). The incorporation of $EMImBF_4$ effectively controls the separation of the graphene layers. Interestingly, an increase in alkyl chain length of the imidazolium salt (with BF_4^- as counterion) results in materials with a larger content of organic compounds and a longer mean-layer spacing.[7] In contrast, imidazolium salts with PF_6^- as counterion or tetraalkylammonium salts, gave a relatively low content of organic material.

Composites of graphene/ionic liquids (G–IL) behave like charge-decorated nanosheets and were assembled alternately with poly(sodium styrenesulfonate) (PSS) by electrostatic LbL adsorption on appropriate solid supports. This procedure provides layered assemblies of G–IL composites with PSS on the surface of a QCM resonator, as indicated by regular shifts of the QCM frequency.[7] The frequency shifts for single adsorption steps roughly correspond to the adsorption of a single G–IL composite layer. Exposure of the composite films to various saturated vapors (25 °C) under ambient conditions after equilibration caused an in situ decrease in frequency of the QCM because of gas adsorption. The amount of adsorbed benzene depends significantly on the type of ionic liquid used, whereas G–water (prepared without an ionic liquid component) showed almost no adsorption capability (Figure 3 a). The G–IL films with a larger content of organic compounds and larger layer spacing, such as G intercalated with G–$HMImBF_4$, tend to have the largest capacity for benzene adsorption.

As clearly indicated in Figure 3 b, the G–$HMImBF_4$ film has superior affinities for aromatic compounds compared to those observed for aliphatic compounds. This behavior is a striking indication of the highly selective detection of aromatic guests within the well-defined π-electron-rich nanospace in the G–IL films. For example, a G–$HMImBF_4$ film showed a significantly higher (more than 10 times) selectivity for benzene vapor than for cyclohexane vapor despite their similar molecular sizes, molecular weights, and vapor pressures (log(pressure/mmHg) values at 25 °C are 1.989 and 1.979 for benzene and cyclohexane, respectively, as calculated from Antoine coefficients[9]). Detection of vapors can be repeated through alternate exposure and removal of the guest solvents (Figure 4 a). Interestingly, a gradual degradation of the on/off response was noted for benzene detection, which is probably caused by the strong interactions between aromatic compounds and the graphene layer, whereas the response to cyclohexane was fully reversible. Responses of the sensor to mixtures of benzene and cyclohexane at different molar ratios showed an approximately linear relation with small cooperative deviations (Figure 4 b), thus facilitating the estimation of gas fractions in mixtures.

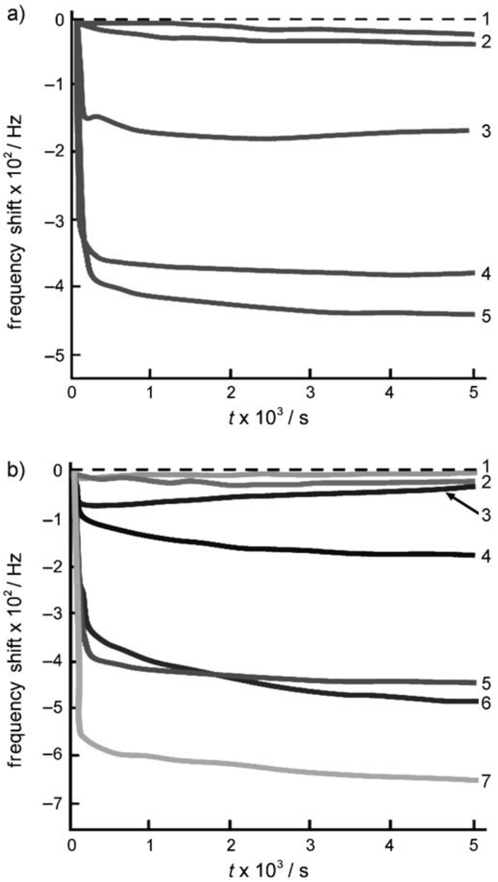

Figure 3. a) QCM frequency shifts upon gas adsorption of benzene to LbL films of 1) G–water, 2) G–$BMImPF_6$, 3) G–$DEMEABF_4$, 4) G–$EMImBF_4$, and 5) G–$HMImBF_4$ at 25 °C. The films were prepared to have similar frequency shifts by using 10–15 LbL cycles. b) QCM frequency shifts upon gas adsorption of 1) hexane, 2) cyclohexane, 3) ethanol, 4) acetone, 5) benzene, 6) pyridine, and 7) toluene to LbL films of G–$HMImBF_4$. The films were prepared by using 10 LbL cycles.

The G–IL films have a variety of potential practical applications that include environment remediation through

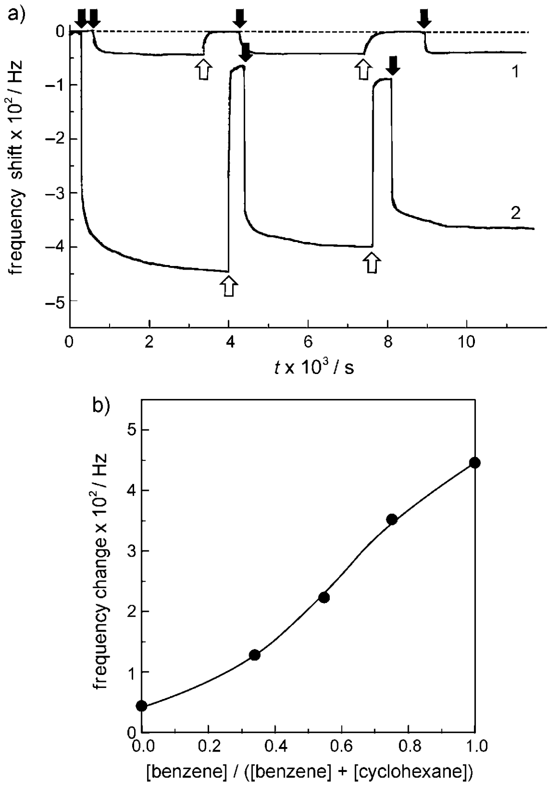

Figure 4. a) QCM sensor responses of a G–HMImBF$_4$ LbL film upon exposure (filled arrows) and removal (open arrows) of guest gas: 1) cyclohexane, 2) benzene. b) QCM changes upon gas adsorption of mixtures of benzene and cyclohexane to a G–HMImBF$_4$ LbL film prepared by 10 LbL cycles.

the capture of atmospheric CO_2. Adsorption of CO_2 vapors from a saturated sodium hydrogen carbonate solution to the G–IL films showed enhanced adsorption volumes compared to G films without intercalated ionic liquids.[7] In addition, control of the electronic properties of the G–IL films upon gas adsorption is possible. The electrical resistance[7] of a G–EMImBF$_4$ film was approximately 178 $\Omega\,sq^{-1}$, and was influenced by gas adsorption, which led to a resistance of, for example, 163 $\Omega\,sq^{-1}$ upon benzene adsorption. This approach enables us to convert gas detection into electrical signals.

To conclude, we have prepared graphene/ionic liquid (G–IL) films by reduction of graphene oxide sheets in the presence of ionic liquids at room temperature and the subsequent LbL assembly. A clear enhancement of aromatic gas adsorption based on increases in graphene layer spacing results in highly selective sensing. The experimental results also indicate a great potential of the G–IL films for practical applications.

Received: August 7, 2010
Published online: November 12, 2010

Keywords: graphene · ionic liquids · layered compounds · layer-by-layer assembly · sensors

[1] a) H. Tsukube, S. Shinoda, *Chem. Rev.* **2002**, *102*, 2389–2403; b) E. A. Meyer, R. K. Castellano, F. Diederich, *Angew. Chem.* **2003**, *115*, 1244–1287; *Angew. Chem. Int. Ed.* **2003**, *42*, 1210–1250; Corrigendum: E. A. Meyer, R. K. Castellano, F. Diederich, *Angew. Chem.* **2003**, *115*, 4254; *Angew. Chem. Int. Ed.* **2003**, *42*, 4120; c) K. Ariga, J. P. Hill, M. V. Lee, A. Vinu, R. Charvet, S. Acharya, *Sci. Technol. Adv. Mater.* **2008**, *9*, 014109.

[2] a) Z. Li, M. Jaroniec, *Anal. Chem.* **2004**, *76*, 5479–5485; b) K. Ariga, A. Vinu, J. P. Hill, T. Mori, *Coord. Chem. Rev.* **2007**, *251*, 2562–2591; c) Y. M. Lvov, D. G. Shchukin, H. Möhwald, R. R. Price, *ACS Nano* **2008**, *2*, 814–820; d) Y. D. Wang, I. Djerdj, N. Antonietti, B. Smarsly, *Small* **2008**, *4*, 1656–1660; e) N. Belman, J. N. Israelachvili, Y. Li, C. R. Safinya, J. Bernstein, Y. Golan, *Nano Lett.* **2009**, *9*, 2088–2093; f) J. P. Paraknowitsch, J. Zhang, D. Su, A. Thomas, M. Antonietti, *Adv. Mater.* **2010**, *22*, 87–92.

[3] a) J. Wu, W. Pisula, K. Müllen, *Chem. Rev.* **2007**, *107*, 718–747; b) E. Yoo, J. Kim, E. Hosono, H. Zhou, T. Kudo, I. Honma, *Nano Lett.* **2008**, *8*, 2277–2282; c) A. H. Castro Neto, F. Guinea, N. M. R. Peres, K. S. Novoselov, A. K. Geim, *Rev. Mod. Phys.* **2009**, *81*, 109–162; d) C.-H. Lu, H.-H. Yang, C.-L. Zhu, X. Chen, G.-N. Chen, *Angew. Chem.* **2009**, *121*, 4879–4881; *Angew. Chem. Int. Ed.* **2009**, *48*, 4785–4787; e) D. R. Dreyer, S. Park, C. W. Bielawski, R. S. Ruoff, *Chem. Soc. Rev.* **2010**, *39*, 228–240; f) Z. Cheng, Q. Li, Z. Li, Q. Zhou, Y. Fang, *Nano Lett.* **2010**, *10*, 1864–1868; g) Y. Song, K. Qu, C. Zhao, J. Ren, X. Qu, *Adv. Mater.* **2010**, *22*, 2206–2210.

[4] a) T. Fukushima, A. Kosaka, Y. Ishimura, T. Yamamoto, T. Takigawa, N. Ishii, T. Aida, *Science* **2003**, *300*, 2072–2074; b) N. Liu, F. Luo, H. Wu, Y. Liu, C. Zhang, Ji. Chen, *Adv. Funct. Mater.* **2008**, *18*, 1518–1525; c) T. Sekitani, Y. Noguchi, K. Hata, T. Fukushima, T. Aida, T. Someya, *Science* **2008**, *321*, 1468–1472; d) S. M. Chen, K. Kobayashi, Y. Miyata, N. Imazu, T. Saito, R. Kitaura, H. Shinohara, *J. Am. Chem. Soc.* **2009**, *131*, 14850–14856; e) F. Chen, Q. Qing, J. Xia, J. Li, N. Tao, *J. Am. Chem. Soc.* **2009**, *131*, 9908–9909; f) B. Zhang, W. Ning, J. Zhang, X. Qiao, J. Zhang, X. Qian, J. Zhang, J. He, C.-Y. Liu, *J. Mater. Chem.* **2010**, *20*, 5401–5403; g) X. Wang, P. F. Fulvio, G. A. Baker, G. M. Veith, R. R. Unocic, S. M. Mahurin, M. Chi, S. Dai, *Chem. Commun.* **2010**, *46*, 4487–4489.

[5] a) N. I. Kovtyukhova, P. J. Ollivier, B. R. Martin, T. E. Mallouk, S. A. Chizhik, E. V. Buzaneva, A. D. Gorchinskiy, *Chem. Mater.* **1999**, *11*, 771–778; b) K. Ariga, J. P. Hill, Q. Ji, *Phys. Chem. Chem. Phys.* **2007**, *9*, 2319–2340; c) J. Shen, Y. Hu, C. Li, C. Qin, M. Shi, M. Ye, *Langmuir* **2009**, *25*, 6122–6128; d) B.-S. Kong, J. Geng, H.-T. Jung, *Chem. Commun.* **2009**, 2174–2176; e) Y. Yan, A. P. R. Johnston, S. J. Dodds, M. M. J. Kamphuis, C. Ferguson, R. G. Parton, E. C. Nice, J. K. Heath, F. Caruso, *ACS Nano* **2010**, *4*, 2928–2936; f) S. Facca, C. Cortez, C. Mendoza-Palomares, N. Messadeg, A. Dierich, A. P. R. Johnston, D. Mainard, J.-C. Voegel, F. Caruso, N. Benkirane-Jessel, *Proc. Natl. Acad. Sci. USA* **2010**, *107*, 3406–3411.

[6] a) W. S. Hummers, R. E. Offeman, *J. Am. Chem. Soc.* **1958**, *80*, 1339–1339; b) S. Stankovich, D. A. Dikin, R. D. Piner, K. A. Kohlhaas, A. Kleinhammes, Y. Jia, Y. Wu, S. T. Nguyen, R. S. Ruoff, *Carbon* **2007**, *45*, 1558–1565.

[7] See the Supporting Information.

[8] a) K. N. Kudin, B. Ozbas, H. C. Schniepp, R. K. Prud'homme, I. A. Aksay, R. Car, *Nano Lett.* **2008**, *8*, 36–41; b) A. C. Ferrari, *Solid State Commun.* **2007**, *143*, 47–57.

[9] G. W. Thomson, *Chem. Rev.* **1946**, *38*, 1–39.